

Proteome wide screen for RNA-dependent Proteins in interphase synchronized HeLa cells

Data Analysis project Summer Term 2022 supervised by Dr. Caudron-Herger

Bolz, C., Bonsen, M., Pott, M., Simon, M.

18.07.2022

Abstract Unraveling the protein-RNA interactome poses a highly dynamic field of research. Several approaches were undertaken and numerous RNA-binding and RNA-interacting proteins have been identified. Harnessing bioinformatics and statistical analysis, we propose a simple and swift way to screen RNA-protein interactome data for RNA-binding proteins obtained by sucrose gradient ultra-centrifugation. We included t-tests, k-means, and linear regression modeling in our analysis. These methods' efficiency is proven by successfully identifying MCM3 as a potential RBP. This was possible because our unique data set consists of HeLa cells synchronized in the interphase of the cell cycle. Furthermore, we confirmed the detection of other previously identified RBPs.

Introduction

RNA and proteins represent a symbiotic system. Proteins need RNA as a template for their biosynthesis as stated by Francis Crick in his "Central Dogma of Molecular Biology" (Crick, 1970). The opposite is also true, studies have shown that proteins need RNA for their catalytic activity, for instance in the RNA-induced silencing complex (Pratt and Macrae, 2009; Wilson and Doudna, 2013). Additionally, some RNA sequences depend on proteins for their synthesis and stability (Kishore *et al.*, 2010). A family of proteins which illustrates this symbiotic relationship are the RNA-binding proteins (RBPs). RBPs present a class of proteins whose interactome depends on RNA. They were shown to play a crucial role in RNA metabolism (Kishore *et al.*, 2010), cancer development (Wei *et al.*, 2022), and genetic disease (Gebauer *et al.*, 2021). Therefore, a deeper understanding of RNA binding and RNA-protein interaction strengthens our ability to adjust and manipulate the cellular mechanisms affected.

RBPs can be categorized into "true" RBPs (e.g. DICER, NPM3), those RNA-binding proteins which directly bind to RNA, and "RBP interacting proteins" which merely interact with "true" RBPs (eg. RBBP7). Furthermore, "true" RBPs can be subcategorized into "RNA-dependent", meaning relying on RNA for their whole and correct function (eg. DICER), and "partially RNA dependent", those that only require RNA for specific functions or transport (eg. NPM3) (Caudron-Herger *et al.*, 2019; Corley *et al.*, 2020).

Several approaches to study RNA-protein interaction and to identify new RBPs were established, such as RaPID and CLIP-Seq. These methods either analyze the interaction between the RNA of interest and additional proteins (RaPID) or the interaction between a protein of interest and the different RNA with which it is interacting (CLIP-Seq) (Qin *et al.*, 2021). Therefore, approaching the global study of RNA-binding protein, interaction networks (Sternburg and Karginov, 2020) has become a matter of interest. A method published by Caudron-Herger *et al.* enables analysis and quantification of whole cell interactomes. Furthermore, this method allows for the identification of new RBPs through RNase treatment and density gradient ultracentrifugation. Subsequently, the resulting fraction shifts of proteins identified via mass

spectrometry were analyzed using bioinformatic techniques (Caudron-Herger *et al.*, 2019, Caudron-Herger *et al.*, 2020).

In this project, we identified RBPs and possible RBP candidates using bioinformatics in R. Beyond that, we further identified contributing variables in our data differentiating RBPs without relying on our entire analysis protocol. We cross-referenced our results with known databases such as R-DeeP (<https://r-deep.dkfz.de/>; Caudron Herger *et al.*, 2019), UniProt (<https://www.uniprot.org/>) and RBP2GO (<https://rbp2go.dkfz.de/>; Caudron-Herger *et al.*, 2021). Our dataset focusing on interphase synchronized HeLa S3 cells were obtained by the method published by Caudron-Herger *et al.* cited above.

Methods

Generation of the dataset

Interphasic HeLa S3 cells were processed as published before (see Caudron-Herger *et al.*, 2019). The data for the amount of protein per fraction, condition, and replicate were collected in arbitrary units and stored in a .csv-file.

Clean-Up and sorting of the dataset

Using the R package tidyverse, two separate data frames were generated containing either all untreated (“_ctrl”) or RNase treated (“_RNA”) replicates. Both data frames, as well as the raw data set, were screened for rows containing zeros only. Those zero rows were removed from the data frame and stored in a new data frame.

Normalization

To rule out batch-to-batch effects and technical error, the protein amounts per replicate (“Rep”) and per fraction (“Frac”) were additionally normalized with respect to each sample. The normalized results were then visualized by plotting the protein distribution in both samples.

Fraction-wise normalization

Normalization for each fraction was performed applying the following equation:

$$Protein(norm) = \frac{maxcolsums}{ColSumme} * Protein(before)$$

Protein(norm) describes the normalized amount of a single protein per fraction and replicate. *ColSumme* represents the total amount of protein per fraction and replicate. For each fraction, one maximum was chosen. *maxcolsums* is the selected maximum total protein amount per fraction and replicate. The parameter *Protein(before)* describes the arbitrary amount of a single protein per fraction and replicate prior to normalization.

Scaling the protein distribution per replicate and condition

For better comparison, the protein amount per fraction was converted to a relative percentage scale by applying the following equation:

$$Protein(relative) = \frac{Protein(norm)}{RowSum} * 100$$

Protein(relative) describes the relative protein amount per fraction in relation to the total amount of the protein per replicate. *Protein(norm)* represents the normalized amount of a single protein per fraction and replicate. The total amount of a single protein per replicate is given by *RowSum*.

Next, data frames for each individual fraction and condition were created, containing the triplicate values for each protein.

Calculation of means with standard deviation

The mean and standard deviation of the triplicates for each protein in each fraction were calculated using the built-in functions *mean()*-(\bar{x}) and *sd()*-*function*(σ) of R. Outliers were detected using $\bar{x} \pm 1\sigma$ as a cut-off. All values below and above the three sigma cut-off were replaced with NA and not considered in the following calculation of the mean.

Shapiro-Wilk Test

To test the normal distribution of the triplicate values, the Shapiro-Wilk test was chosen due to its high power in small populations compared to other tests. The test was performed using the built-in R function *shapiro_test()*.

Determination of Maxima

We determined the global maximum for the RNase-treated and untreated samples for all proteins. The protein content (y-value) was compared to the two neighbors right and left of the analyzed fraction (x-position). For fractions 1 and 25, only the neighbors right or left of the fraction could be compared due to border limitations. For fractions 2 and 24 only one neighbor could be compared left or right. Obtained values were stored in a separate data frame.

Detection of Protein Shifts

In our analysis, we considered shifts in the global maximum by comparing RNA-treated and untreated samples as a proxy for the presence of RNA. We required “shifting proteins” to show both a significant x-shift and y-shift to improve precision.

X-shifts

First, we compared the x-position of the global maximum in both samples. To quantify the shift, we determined the difference in the fraction number of the control group and the RNase-treated sample.

$$x - shift = |fracs_max_ctrl| - |fracs_max_RNase|$$

The variables *fracs_max_ctrl* and *fracs_max_RNase* describe the x-position of the global maxima for control and RNase treatment respectively. *x-shift* is the resulting value and used for shift-direction determination.

The following convention regarding x-shifts was used:

1. Left-shift: Value < 1
2. Right-shift: Value > 1
3. No-Shift: Value = 0

Y-shifts

The total value of the y-shift was calculated as the difference between the y-values of the global maxima for both conditions.

$$y - shift_total = |absolute_max_ctrl| - |absolute_max_RNase|$$

The variables *absolute_max_ctrl* and *absolute_max_RNase* describe the y-value of the global maxima for control and RNase treatment respectively. *y-shift_total* is the resulting value.

Statistical analysis

To identify significant y-shifts, we used statistical analysis to determine the difference in the relative protein amount (y-value) for each protein in the global maximum fraction of RNase-treated and untreated samples. All proteins with x-shift values $\geq |1|$ were considered.

F-Test

To determine whether our sample variances were comparable and therefore suitable for the two-tailed, unpaired t-test, a two-sided F-Test was performed on the triplicates of each protein and fraction using the built-in R function *var.test()*. The significance level (p-value) was set to $\alpha = 0.01$. The test was deemed positive if $p - value > 0.01$.

If *var.test()* was performed on all zero samples, NA/NaN was returned. Therefore, the F-test filtered out those samples that were not relevant for maxima analysis anyways. Since only the comparison of y-values at the x-positions of the global maxima mattered for our further analysis, proteins that failed the F-test (p-value < 0.01) at those x-positions were excluded. To quantify how many proteins failed F-test RNase- and ctrl-maximum spots were analyzed. To refer the F-test results back to the actual proteins, a more visual matrix was created labeled *p_value_matrix*.

Students T-Test

The two-tailed, unpaired t-test was used to identify proteins with significant y-value changes in global maxima x-positions after treatment. P-Values were calculated for each triplicate per protein per fraction using the built-in R function *t.test()*. Fractions with a global maximum were compared to the significance level $\alpha = 0.05$. The test was deemed positive if $p - value < 0.05$. Therefore, the change was considered significant.

Since the t-test was performed on y-values of x-positions of global maxima for both conditions separately, the returned results were either TRUE/TRUE, TRUE/FALSE, FALSE/TRUE or FALSE/FALSE for the ctrl and RNase maxima. Only proteins with positive t-tests (p-value < 0.01) for the global maximum in both conditions (TRUE/TRUE) were considered for further analysis.

Identification of potential RBPs by analysis of x- and y-shift

Potential RBPs were selected by filtering out proteins with significant y-shifts following the t-test but no significant x-shift in the global maxima fractions. The Cut-off condition was defined as significant y-shift and x-shift > 1 .

Proteins filtered out by this method were removed from the data frame and stored separately for further analysis.

Checking for false positive and false negative results

False-positive and false-negative proteins were determined by cross-referencing with two data sets which were provided by Maiwen Caudron-Herger at Prof. Dr. Sven Diederichs Lab (DFKZ) (unpublished data). The data contains information on RBPs and non-RBPs previously identified by different researchers.

Precision is defined as:

$$precision = \frac{TP}{TP + FP}$$

Accuracy is defined as:

$$accuracy = \frac{TP + TN}{TP + TN + FP + FN}$$

TP = True positives, FP = False positives, TN = True negatives, FN = False negatives

Identification of potential RBD Proteins

Potential RNA-binding dependent (RBD) protein candidates were identified by cross-referencing false-positive proteins with the data set provided by Maiwen Caudron-Herger at Prof. Dr. Sven Diederichs Lab (DFKZ) (unpublished data).

k-means clustering

Using the libraries *corrplot*, *cluster* and *factoextra*, k-means clustering was conducted using the k-means algorithm. First, we defined a function that calculates the quotient by the following equation for all proteins.

$$Quotient = \frac{mean_RNase(Protein)}{mean_ctrl(Protein)}$$

The resulting values were stored in a matrix labeled *q_Hela_mat*. *mean_RNase(Protein)* describes the mean value for each protein and fraction in the RNase treated sample. *mean_ctrl(Protein)* describes the mean value for each protein and fraction in the ctrl sample. Then, we selected the maximum value (*maxi_RNase*) for each protein and calculated the overall quotient sum (*q_mat_sums*) for each protein and sample. These values were stored in the data frame *abs_max_both_q*.

Using the *factoextra* function *fviz_nbclust()* we created a silhouette plot to determine the optimal cluster number. With the built-in R function *k-means()* we clustered our proteins using the previous determined variables *q_mat_sums* and *maxi_RNase* into three clusters.

Cluster A: Non-shifter

Cluster B: Potential shifter

Cluster C: Sure-shifter

To check the quality of our clustering, we created another silhouette plot using *factoextra*. To check our clustering results, we cross-referenced our determined RBP using our four functions including *Find_true_RBP*.

Linear regression analysis

To train our linear regression model, we selected 5000 random proteins from our raw data set. For these proteins, we took the values *maxi_RNase* and *q_mat_sums* from the data frame *abs_mat_both_q*. We created a model to predict the x-shift based on those values. To test our regression model, the remaining 2081 proteins were analyzed by the model. We cross-referenced the results with the data provided by Maiwen Caudron-Herger.

Results

Clean-Up and normalization

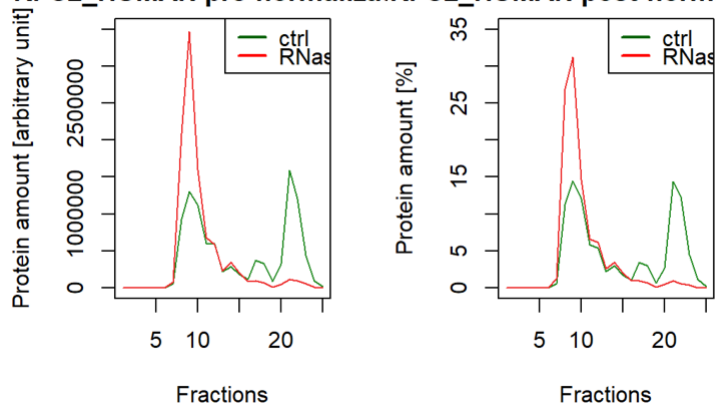
The initial data set consisted of 7086 proteins. After clean-up, 7081 proteins remained for further analysis. Normalization was visualized for several reported sure-shifters and non-shifters (see Caudron-Herger *et al.*, 2019). The selected proteins were:

Sure-shifters: Sin3A_HUMAN, HDAC1_HUMAN, HNRPU_HUMAN, RFC2_HUMAN

Non-shifters: ASNS_HUMAN, MCM2_HUMAN, MCM3_HUMAN

Through normalization, the arbitrary values were converted into a relative percentage scale. Yet, the overall distribution of the protein amount per fraction remained comparable to the distribution prior to normalization. Therefore, the normalization worked for sure-shifters as well as non-shifters. For instance, figure 1 displays the normalization of a sure-shifter (RFC2_HUMAN) and a non-shifter (MCM2_HUMAN).

A RFC2_HUMAN pre-normalizatRFC2_HUMAN post-normaliza



B MCM2_HUMAN pre-normalizaMCM2_HUMAN post-normaliza

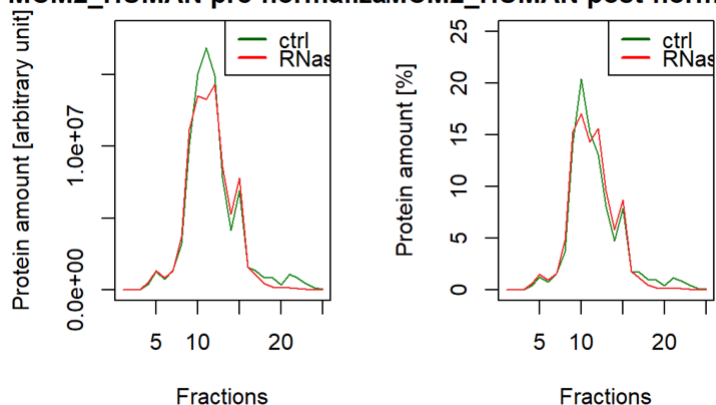


Figure 1: Comparing pre- and post-normalization (A): Comparison of the sure-shifter RFC2_HUMAN prior to and post-normalization. (B): Comparison of the non-shifter MCM3_HUMAN prior to and post normalization. For both selected proteins, the overall trend of distribution remains comparable.

Calculation of mean with sd and Shapiro-Wilk Test

With the proposed 1σ cut-off, we excluded a single value for 122175 triplicates. The Shapiro-Wilk test concluded that all replicate values obtained were normally distributed for both samples. Therefore, we found the data suitable for statistical analysis with the F-Test and two-tailed unpaired T-test.

Statistical analysis and Identification of potential RBPs by analysis of x- and y-shift

The obtained x- and y-shifts, as well as the fractions of the global maxima, shift directions and y-shift values were stored in a data frame labeled *abs_max_both*.

7081 proteins were tested with the F-Test. Only the obtained p-values for global maxima fractions were deemed relevant for the identification of potential RBP candidates. Of 7081 proteins, 1196 failed the F-test and were excluded from further analysis. 5885 remained. Quantification of FALSE results in the F-Test showed, that 10 % of all analyzed proteins failed the F-Test. This means that either one or both triplicates' variances at global maxima positions vary. Because some FALSE F-test results may originate from outlier values (see discussion) and otherwise we would have had to exclude too much of our data, the significance level was set to $\alpha = 0.01$ instead of the previously used $\alpha = 0.05$. With $\alpha = 0.01$, closer to 5 % of the data was excluded based on a FALSE F-test result. With this compromise, some likely faulty data was still excluded, while we retained as much data for further analysis as possibly arguable.

The two-tailed unpaired t-test was applied to the remaining 5885 proteins per triplicate in the ctrl vs RNase treatment. P-Values were checked for significance at previously determined maxima positions. We identified 2929 potential shifters. Only 5838 proteins were annotated in the data set used for cross-referencing. The RBP prediction of these 5838 proteins was analyzed. The x-shift > 1 cut-off allowed us to identify 513 true RBP (TP) with 121 false positives (FP) out of 634 identified RBP in total. Of the 121 false positives, six were identified via cross-referencing as RBD proteins. 5214 proteins were predicted as non-RBP. Cross-referencing revealed, that 3600 proteins were false-negatives (FN) and 1614 were true-negatives (TN). This results in a precision of 80.914 % and an accuracy of 36.43 % (see **Fig.2C**)

With the t-test-based analysis, we detected one out of four previously selected sure-shifters and all non-shifters. Additionally, MCM2_HUMAN - a believed non-shifter - was identified as an RBP with a significant shift (see **Fig.4D**).

K-Means Clustering

The clustering analysis concluded that 73.88 % of our data was represented. Values were assigned with 81 % accuracy to our cluster.

The clustering analysis was conducted with three clusters (see **Fig. 2B**). For cluster 1 (in methods as cluster C) 53 true RBP (TP = 96.4%) and 2 false RBP (FP = 3.6%) were detected. Cluster 2 (B) presented a similar accuracy of 318 true RBP (TP = 96.7%) and 10 false RBP (FP = 3.1%). Therefore, we decided to combine clusters B and C, as both accurately predicted true RBPs.

For the combined cluster BC, 384 RBP were identified. 371 (TP = 96,6%) were true RBP and 12 false RBP (FP = 3,1%) were found. One RBD was detected out of the false-RBP proteins. For cluster 3 (A) 2557 true non-RBP (TN = 38.2%) and 4089 false non-RBP (FN =61.1%) were detected. The results are displayed in **Fig. 2C**. This results in a precision of 96.87 % and an accuracy of 41.66 %.

With the clustering, we detected none of our previously selected sure-shifters and all non-shifters.

Linear Regression model

Since the regression takes different random proteins for the training every time, the shown results were generated once. $R^2 = 0.2266$. Out of 2081 tested proteins, 883 RBP were predicted of which 525 (TP = 59,4%) turned out as true RBPs and 347 (FP = 39,3%) were false RBPs. 1198 non-RBPs were predicted. 470 (TN = 39.2%) were true non-RBPs while 709 (FN = 59.2%) were false non-RBPs. 8 RBDs were detected out of the false-RBP proteins. The results are displayed in **Fig. 2C**. This results in a precision of 60.21 % and an accuracy of 48.51 %. With the regression, we detected none of our previously selected sure-shifters and one out of three non-shifters.

Connecting Statistical analysis, Clustering and Linear Regression

All three methods identified the same 2979 RBPs or non-RBPs respectively. The overlap of all three methods consists of 728 true RBP, 483 false RBP, 715 true non-RBP, and 1032 false RBP.

The most overlap of classified proteins is found in the comparison of the clustering and statistical tests. The same 5259 (compared to 3310 and 4470) proteins were identified as RBPs or non-RBPs respectively. The overlap of clustering and statistical test results consists of 182 true RBP, 9 false RBP, 1623 true non-RBP, and 3415 false RBP.

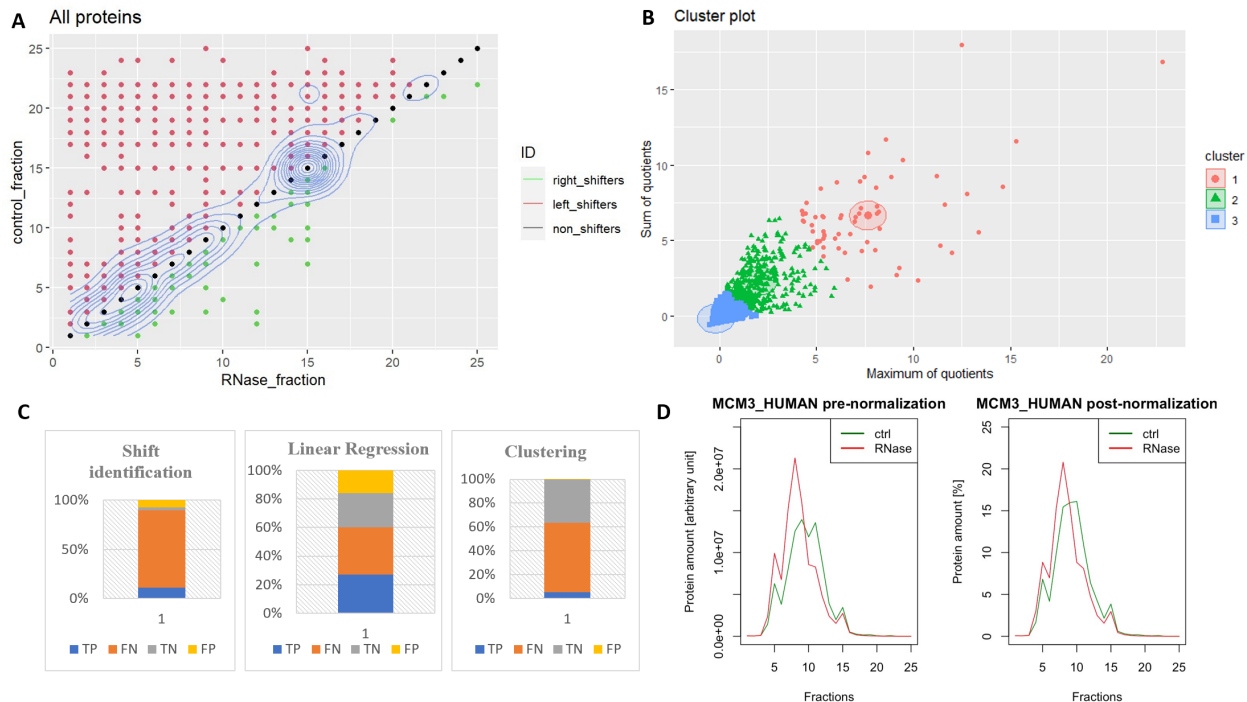


Figure 3: Overview of obtained results (A) Plot of all 7081 proteins, calculated global maxima were plotted against each other, proteins can be classified as either right-shifter (green), left-shifter (red) or non-shifter (black). Density (blue) indicates that most proteins are non-shifters. (B) k-means clustering of our proteins as described in methods, three distinct clusters can be visualized, Cluster 1 = sure-shifters (red), Cluster 2 = possible shifters (green), Cluster 3 = non-shifters (blue). (C) Overview of identification results for Shift based identification = Shift identification, Linear Regression model and k-means clustering. (D) Pre and post-normalization plot of MCM3_HUMAN, clearly showing the occurring shift.

Discussion

Our methods detect potential RBPs that shift more than one fraction and accumulate in a single fraction after treatment with RNase. However, we detected absolute x-shifting values only because we decided against smoothing our data and did not apply a Gaussian fit model. Therefore, we were not able to detect RBPs that shift fewer than one absolute but more than zero fractions, for example, RBP2_HUMAN. On R-Deep, RBP2_HUMAN is listed as an RBP but only shifts 0.1 fractions. Our method failed to detect this marginal shift.

Possibly, we also did not detect this protein because the chosen sample preparation method was not suitable. A more distinguished density gradient consisting of more than 25 fractions could have potentially resulted in a higher resolution. Hence, the shift could have been detected.

Furthermore, we applied our selection method to global maxima only. This resulted in the inability of identifying proteins that mainly accumulated in local maxima fractions. Our method also failed to detect proteins, where the global maximum is not the shifting fraction upon treatment with RNase, resulting in a TRUE/FALSE y-shift in the t-test. This applied for HDAC1_HUMAN (see R-Deep Database). We were left with a moderate precision (80.91 %) and low accuracy when identifying RBPs via statistical tests.

In comparison, our clustering had the highest precision (96.87 % compared to 80.91 % and 60.21 %) of all applied methods. Therefore, proteins that were located in Cluster B and C precisely identified RBPs. Not all RBPs were located in those two clusters which displayed our poor accuracy of 41.66 %. Perhaps, the accuracy of the clustering could be enhanced by choosing other clustering variables.

The trained linear regression model worked with low precision of 60.21 % and low accuracy of 48.51 %. This

was caused by the insufficient R^2 of 0.2266 resulting in severe underfitting. Consequently, the assignment as RBP or non-RBP for the 2081 proteins tested lacked sophistication. Since the proteins are randomly selected, RBPs might be over- and under-represented in the training cohort of our model.

Most of the identified RBPs plus the identified non-RBPs do not add up to 100 %. This is because proteins listed in the provided data sets were cross-referenced only. For this reason, some potential RBPs were not evaluated and therefore not properly classified.

Overall, the three methods - statistical tests, clustering and regression - deliver the same classification for almost half of all analyzed proteins. This shows once more that all methods fail to identify the same proteins as well. It must therefore not be an error in the methods, but the data input. As previously highlighted, the data input could be improved by adding a Gaussian fit etc.

The most similar results with 5259 shared classifications were returned by the comparison of the clustering and statistical tests. As a cross-reference, both methods seem to validate one another. On the other hand side, this shows that the clustering poses a viable short-cut compared to the extensive statistical tests. With the greatest precision of 96.87 %, clustering may deliver more reliable results than the statistical tests in fact. However, the total amount of identified true RBPs is fewer in the clustering with 371 compared to 508.

Looking back at our previously selected and classified sure-shifters and non-shifters - Sin3A_HUMAN, HDAC1_HUMAN, HNRPU_HUMAN, RFC2_HUMAN and ASNS_HUMAN, MCM2_HUMAN, MCM3_HUMAN - all are listed as RBPs on R-DeeP. However, some were classified as non-shifters by Caudron-Herger *et al.*. Our method detected one of those proteins formerly classified as a non-shifter - RBP MCM3_HUMAN.

MCM3 is part of the MCM2-7 helicase complex which enables DNA replication during the S-Phase (Todorov *et al.*, 1994) of the cell cycle. The DNA replication complex is associated with topoisomerase I which interacts with RNA when replication stalls or strand breaks during the unwinding of the DNA strands occur (Takisawa *et al.*, 2000). Our data set was derived from HeLa cells synchronized in the interphase. The interphase consists of the G_1 , G_2 , and S-Phase (Malumbre & Barbacid, 2009). Therefore, it is plausible that expression levels of proteins playing a role in these phases such as MCM3 are elevated. RNA interaction would be present allowing for detection by our proposed methods.

In conclusion, our method is suitable for the identification of RBPs. We were able to identify previously identified RBPs with moderate accuracy and high precision. Additionally, we detected at least one RBP which was not previously mentioned in our methods. With the proposed changes such as a Gaussian fit, the accuracy could potentially be improved. Our technique proposes a simple, swift, initial way for analysis of ultra-centrifugation data but provides poor accuracy. For further analysis, a more accurate and precise method needs to be developed.

References

- Caudron-Herger, M., Jansen, R.E., Wassmer, E., and Diederichs, S. (2021). RBP2GO: a comprehensive pan-species database on RNA-binding proteins, their interactions and functions. *Nucleic Acids Research* 49.
- Caudron-Herger, M., Rusin, S.F., Adamo, M.E., Seiler, J., Schmid, V.K., Barreau, E., Kettenbach, A.N., and Diederichs, S. (2019). R-DeeP: Proteome-wide and Quantitative Identification of RNA-Dependent Proteins by Density Gradient Ultracentrifugation. *Molecular Cell* 75, 184-199.
- Caudron-Herger, M., Wassmer, E., Nasa, I., Schultz, A.-S., Seiler, J., Kettenbach, A.N., and Diederichs, S. (2020). Identification, quantification and bioinformatic analysis of RNA-dependent proteins by RNase treatment and density gradient ultracentrifugation using R-DeeP. *Nature Protocols* 15, 1338-1370. 10.1038/s41596-019-0261-4.
- Corley, M., Burns, M.C., and Yeo, G.W. (2020). How RNA-Binding Proteins Interact with RNA: Molecules and Mechanisms. *Molecular Cell* 78, 9-29.
- Crick, F. (1970). Central Dogma of Molecular Biology. *Nature* 227, 561-563.
- Gebauer, F., Schwarzl, T., Valcárcel, J., and Hentze, M.W. (2021). RNA-binding proteins in human genetic disease. *Nature Reviews Genetics* 22, 185-198.
- Kishore, S., Lubner, S., and Zavolan, M. (2010). Deciphering the role of RNA-binding proteins in the post-transcriptional control of gene expression. *Briefings in Functional Genomics* 9, 391-404.
- Li, W., Deng, X., and Chen, J. (2022). RNA-binding proteins in regulating mRNA stability and translation: roles and mechanisms in cancer. *Seminars in Cancer Biology*.
- Malumbres, M., and Barbacid, M. (2009). Cell cycle, CDKs and cancer: a changing paradigm. *Nature Reviews Cancer* 9, 153-166.
- Mullari, M., Lyon, D., Jensen, L.J., and Nielsen, M.L. (2017). Specifying RNA-Binding Regions in Proteins by Peptide Cross-Linking and Affinity Purification. *Journal of Proteome Research* 16, 2762-2772.
- Pratt, A.J., and Macrae, I.J. (2009). The RNA-induced Silencing Complex: A Versatile Gene-silencing Machine. *Journal of Biological Chemistry* 284.
- Qin, W., Cho, K.F., Cavanagh, P.E., and Ting, A.Y. (2021). Deciphering molecular interactions by proximity labeling. *Nature Methods* 18, 133-143.
- Sternburg, E.L., and Karginov, F.V. (2020). Global Approaches in Studying RNA-Binding Protein Interaction Networks. *Trends in Biochemical Sciences* 45, 593-603.
- Takisawa, H., Mimura, S., and Kubota, Y. (2000). Eukaryotic DNA replication: from pre-replication complex to initiation complex. *Current Opinion in Cell Biology* 12, 690-696.
- Todorov, I.T., Pepperkok, R., Philipova, R.N., Kearsey, S.E., Ansorge, W., and Werner, D. (1994). A human nuclear protein with sequence homology to a family of early S phase proteins is required for entry into S phase and for cell division. *Journal of Cell Science* 107, 253-265.
- Wilson, R.C., and Doudna, J.A. (2013). Molecular Mechanisms of RNA Interference. *Annual Review of Biophysics* 42, 217-239.